Reflectance Modification in Nanostructured Silicon Layers with Gradient Porosity

G. K. Mussabek[a,b], D. Yermukhamed[a], Z. A. Suleimenova[a], R. B. Assilbayeva[c], V. A. Sivakov[d], I. N. Zavestovskaya[b,e*], and V. Yu. Timoshenko[b,e,f]

[a] *Al-Farabi Kazakh National University, 71 al-Farabi Ave., 050040 Almaty, Kazakhstan*
[b] *National Research Nuclear University "MEPhI", Institute of Engineering Physics for Biomedicine,*
*31 Kashirskoe Sh., 115409 Moscow, Russia; *e-mail: inzavestovskaya@mephi.ru*
[c] *Yessenov Caspian State University of Technology and Engeenering,*
Mangistau region, 32th Microdistrict, 130003 Aktay, Kazakhstan
[d] *Leibniz Institute of Photonic Technology, 9 Albert-Einstein St., 07745 Jena, Germany*
[e] *Lebedev Physical Institute, Russian Academy of Sciences,*
53 Leninskii Pr., Moscow, 119991 Russia
[f] *Faculty of Physics, Moscow State University, 119991 Moscow, Russia*
Received July 24, 2019; in final form, October 4, 2019; October 10, 2019

Abstract—A significant change in effective reflectance spectra of nanostructured porous silicon layers grown with different times of metal-assisted chemical etching is detected. The low reflectances at the level of 5−10% measured in the spectral range of 200−400 nm are explained by strong elastic scattering of light in combination with absorption in silicon nanostructures, while a reflectance increase in the range of 500−1800 nm, which is visually detected as a "white" layer appearance is associated with Mie scattering in silicon nanostructures with gradient porosity under conditions of weak optical absorption. The results obtained are discussed from the viewpoint of potential applications of "black" and "white" nanocrystalline silicon in photonics and sensorics.

Introduction. Recently, methods for fabricating nanostructures based on chemically pure silicon (Si) [1−3] for applications in photonics [2], photoelectric devices [4, 5], energy storage devices [6], biophotonics [3, 7], and biosensorics [8] have been intensively developed. The method of metal-assisted chemical etching (MACE) of single-crystal silicon wafers (c-Si), which is based on selective dissolution of silicon in fluoric acid solutions, assisted by metal (as a rule silver) nanoparticles, makes it possible to grow silicon nanostructures with different morphologies and tailored optoelectronic properties [9]. On the one hand, good control of the silicon nanostructure morphology can be achieved by varying the etching conditions and initial c-Si substrate parameters during MACE [9−11]. On the other hand, despite numerous studies devoted to the optical properties of the nanostructures fabricated by the MACE method [9, 12], there are still some questions associated with the effect of porosity and complex morphology exhibiting fractal dimensionality [13] on light reflection and absorption. The objective of this work is to study the effect of the porosity gradient of nanostructured layers grown by the MACE method on their optical properties in the ultraviolet (UV), visible, and near-infrared (NIR) spectral regions.

Objects under study and research technique. Nanostructured porous silicon (PSi) layers were obtained by the two-step MACE method using silver nanoparticles as a catalyst [9]. As substrates, (100) c-Si wafers with optically polished surfaces, *p*-type conductivity, and resistivity of 1−10 Ω·cm were taken. As an etching solution, a mixture of an aqueous solution of fluoric acid (5 mol/l) and hydrogen peroxides (33%) with the volumetric ratio of 8:1 was used. PSi layers of different thicknesses were obtained by varying the etching time from 1 min to 10 hours. Residual silver nanoparticles were removed by placing the obtained layers in concentrated nitric acid for 15 min, followed by washing and drying in air. The prepared samples were studied using an ULTRA 55 FE-SEM (Carl Zeiss) scanning electron microscope (SEM). The spectra of total (combined diffuse and specular) reflections were measured in
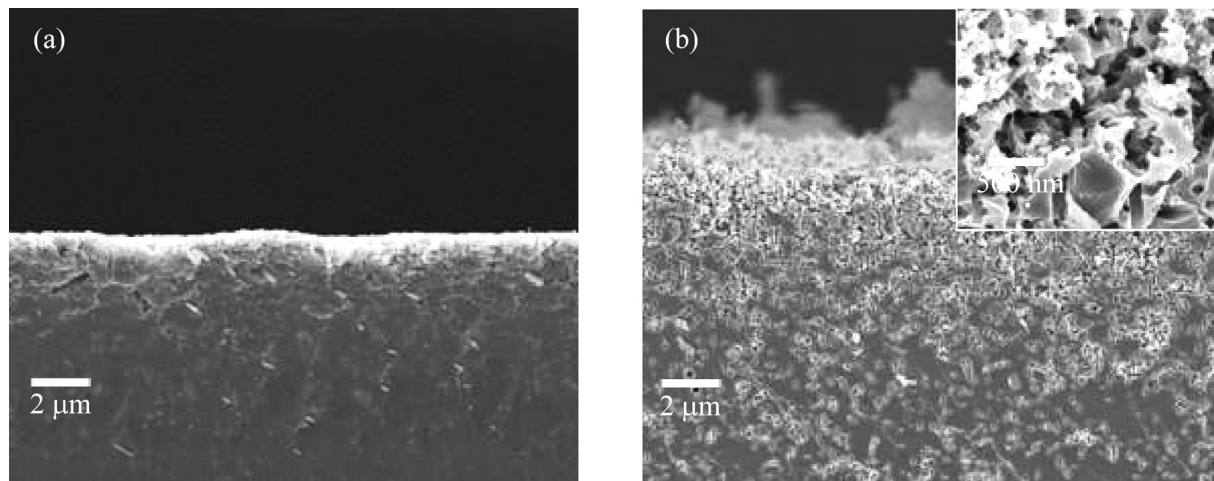
Fig. 1. SEM images of the cross section of the PSi layers fabricated by the MACE method with formation times of: (a) 60 min and (b) 600 min. The inset in panel (b) shows the magnified image of the PSi layer surface.

the optical range from 200 to 1800 nm using a V-770 (Jasco) spectrophotometer with a 60-mm ISN-923 integrating sphere. Optical measurements were performed at room temperature in air.

Results and discussion. Figure 1 shows the typical SEM images of the cross section of the PSi layers grown with various etching times. The samples had a mesoporous structure with gradient porosity, i.e., the top layer was more porous, and the number of pores decreased toward the substrate. The PSi layer thickness was estimated from the SEM images. The dependence of the PSi layer thickness on the formation time exhibits a sublinear dependence with the tendency to flattening at times larger than 10 min. A decrease in the PSi layer growth rate with time can be explained by ion diffusion inhibition in the formed porous structure [9].

Figure 2(a) shows the total reflection spectra for samples fabricated with various MACE times. We can see low (5−10%) reflectances in the UV region and an increase in the reflectance in the near IR region; in this case, the effect strongly depends on the layer thickness. The samples of PSi layers formed
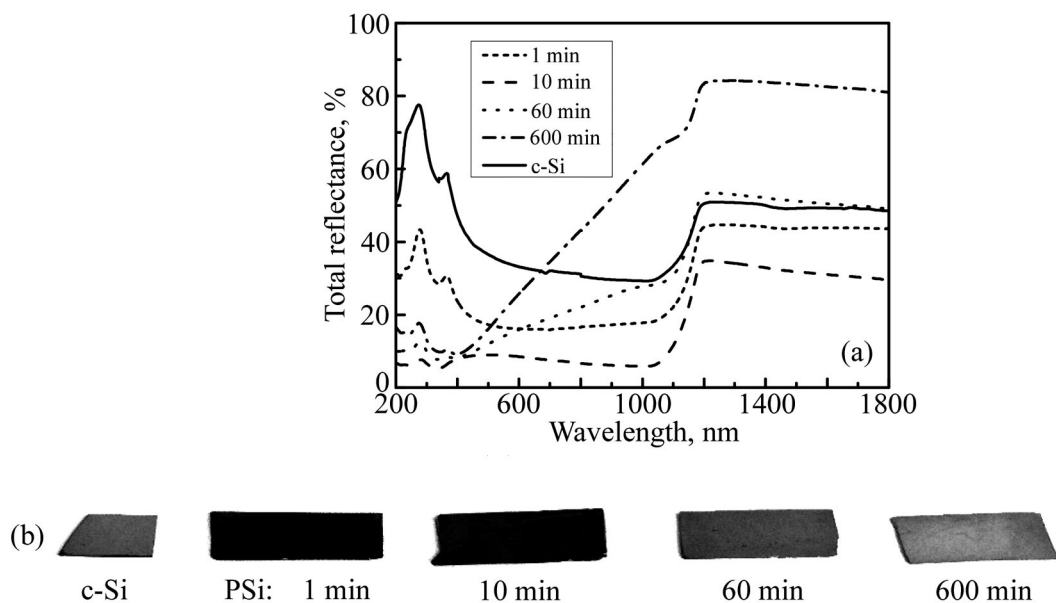

Fig. 2. (a) Total (specular and diffuse) reflection spectra of PSi layers for various MACE times and, for comparison, the spectrum of the c-Si substrate, and (b) digital images of initial c-Si wafer samples and surfaces of PSi layers fabricated with MACE times (from left to right) from 1 to 600 min.
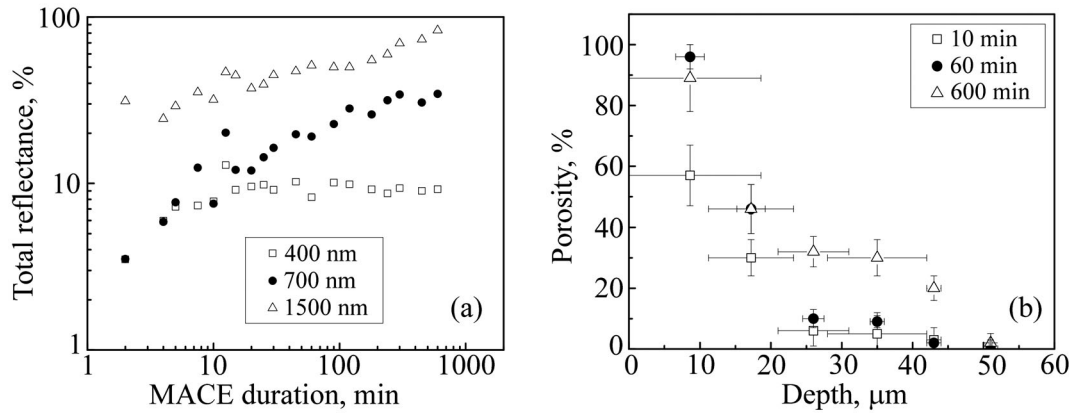
Fig. 3. (a) Dependences of the total reflectances measured at wavelengths of 400 (squares), 700 (circles), and 1500 nm (triangles) on the formation time of PSi layers; (b) porosity profiles over the layer depth, obtained by analyzing the corresponding SEM images.

for times from 1 to 10 min exhibit the reflectance below 5% in the UV spectral region. This can be explained by partial localization of light due to its strong elastic scattering accompanied by absorption in Si nanocrystals [15]. For the PSi samples thicker than 20 μm, light scattering observed in the spectral region above 1 μm corresponds to weak absorption and probably causes the high total reflectance, up to 90%. It should be noted that thin PSi layers looked like the so-called "black" silicon, while the samples thicker than 10 μm showed bright color (see Fig. 2(b)). The "black" to "white" transition of the surface was observed at a PSi layer thickness over 20 μm.

As seen in Fig. 2(a), for the PSi layers formed for 60 min and longer, an increase in the reflectance is observed in the range of 500−1200 nm. This feature can be attributed to Mie scattering in Si nanostructures with sizes comparable to the light wavelength [16]. The number of scattering centers in the form of nanocrystalline silicon regions from 100 to 500 nm in size increases with the PSi layer thickness (see the inset in Fig. 1(b)), which results in the enhancement of Mie backscattering [17]. This explains the reflection enhancement in the visible and near IR spectral regions (see Fig. 2(a)), which is visually detected as the "white" layer appearance (see Fig. 2(b)).

The transformation of the PSi optical properties from "black" to "white" silicon is also seen from the dependences of the total reflectance in the presence of strong, medium, and weak absorption, i.e., for wavelengths of 400, 700, and 1500 nm, respectively (see Fig. 3(a)). Although in the UV spectral region, the total reflectance does not change significantly, its value for the wavelength of 1500 nm gradually increases to 80% with the MACE time. This indicates the appearance of a large number of light scatterers with average sizes larger than 100 nm [17].

To determine the role of the morphology of the PSi layers in the changes in their optical properties, the numerical analysis of the corresponding SEM images was performed using the approach proposed in [13]. In particular, the SEM images were transformed into a "black-and-white" digital format, which allowed us to estimate the porosity according to the expression

$$P = Nb/(Nb + Nw), \tag{1}$$

where Nb and Nw are the numbers of black (pores) and white (silicon nanocrystals) pixels.

It follows from the analysis by relation (1) that the porosity of the top layer significantly increases with the formation time (Fig. 3(b)), which indicates processes of additional dissolution of silicon nanocrystals during the growth of PSi layers [12].

To estimate the porosity gradient of the samples under study, the corresponding SEM images of the cross sections of the PSi layers were analyzed. To this end, the images were divided into strip regions (with a width of 2−5 μm) from the surface to the interface with the c-Si substrate. These regions were processed using relation (1). The numerical analysis of the images indicates a decrease in the porosity from the maximum value of about 80−90% at the layer top to minimum values at the PSi/c-Si interfaces, as shown in Fig. 3(b). In particular, the porosity of the PSi layer obtained by 600-min MACE decreases from 90% on the surface to 20% at a depth of 45 μm.
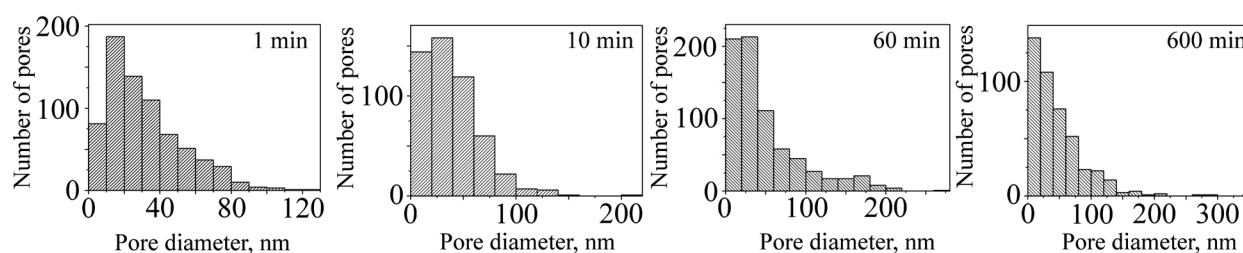
Fig. 4. Pore size distributions constructed by analyzing the SEM images of the surfaces of PSi layers grown with various MACE times.

To determine the pore diameters and the pore size distribution, a numerical analysis of the SEM images of the PSi layer surfaces using the Image J software package was also performed. Figure 4 shows the pore size distributions for the top layers of the PSi samples. In the case of the samples formed for relatively short MACE times (1−10 min), the formation of smaller pores, 20−30 nm in diameter on average, is observed. However, the layer formation for a longer time (from 1 to 10 hours) results in the formation of larger pores 50−60 nm in diameter. The average number of pores decreases with PSi layer thickening due to Si dissolution and macropore formation. An increase in the pore sizes during etching can be explained by the dissolution of Si walls between primary pores due to repeated precipitation of silver nanoparticles from the etching solution [18].

The results obtained point to a simple method for modifying photonic properties of silicon nanostructures in a wide range, which can be useful for various applications. For example, "black" silicon obtained by metal-assisted chemical etching of silicon can be used to increase the efficiency of silicon solar cells [5, 19]. We note that the minimum reflectance in the visible and near IR spectral regions for the samples obtained in this study slightly exceed the similar values for "black silicon" formed by nanostructuring silicon surfaces by pico- and femtosecond radiation in a sulfur fluoride atmosphere developed by E. Mazur's research team (see, e.g., in [20]). At the same time, the metal-assisted chemical etching procedure used in the present study, when choosing corresponding parameters, can also yield extremely low (less than 5%) reflectances in the spectral region under consideration [7]. Furthermore, in comparison with the "black silicon" formation method [20], the MACE method is simpler, relatively inexpensive, allows simultaneous processing of the entire surface of c-Si wafers of any diameter and does not lead to contamination of nanostructured silicon layers by sulfur or other impurities [9]. Furthermore, as follows from the above results, this method makes it possible to produce "white silicon" which can be recommended as a matrix for lasing under conditions of strong scattering (so-called "random lasing" [21]). Moreover, "white silicon" can be useful for applications in sensorics in optical diagnostics of active molecules whose adsorption on the surface causes changes in the free carrier concentration in nanocrystals [22]. Light absorption by free carriers will increase losses during multiple light scattering, which will decrease the diffuse reflectance of nanosilicon layers.

Conclusions. The results obtained suggest that the low reflectance of thin porous silicon layers formed by metal-assisted chemical etching of single-crystal silicon wafers in fluoric acid solutions can be explained by light scattering accompanied by efficient absorption in silicon nanostructures. At the same time, increased total reflection in the visible and IR spectral regions is explained by light scattering in the silicon nanostructures with gradient porosity under conditions of low light absorption.

REFERENCES

1. A. A. Ischenko, G. V. Fetisov, and L. A. Aslalnov, *Nanosilicon: Properties, Synthesis, Applications, Methods of Analysis and Control* (CRC Press, USA, 2014).
2. D. Thomson, A. Zilkie, J. E. Bowers, et al., J. Opt. **18**, 07300 (2016).
3. V. Yu. Timoshenko, Phys. Sci. Technol. **4**, 59 (2017).
4. S. Wipperman, Y. He, M. Voros, and G. Galli, Appl. Phys. Rev. **3**, 040807 (2016).
5. H. Savin, P. Repo, G. von Gastrow, et al., Nat. Nanotechnol. **10**, 624 (2015).
6. J.-K. Yoo, J. Kim, H. Lee, et al., Nanotechnol. **24**, 424008 (2013).
7. L. A. Osminkina, V. Sivakov, G. A. Mysov, et al., J. Biophotonics **5**, 529 (2014).
8. S. Dhanekar and S. Jain, Biosens. Bioelectron. **41**, 54 (2013).
9. Zh. Huang, N. Geyer, P. Werner, et al., Adv. Mater. **23**, 285 (2011).
10. M.-L. Zhang, K.-Q. Peng, X. Fan, et al., J. Phys. Chem. C **112**, 4444 (2008).
11. H. Han, Zh. Huang, and W. Lee, Nano Today **9**, 271 (2014).
12. A. Ghafarinazari and M. Mozafari, J. Alloys Compd. **616**, 442 (2014).
13. B. Fazio, P. Artoni, M. A. Iati, et al., Light: Sci. Appl. **5**, e16062 (2016).
14. X. Li and P. W. Bohn, Appl. Phys. Lett. **77**, 2572 (2000).
15. L. A. Osminkina, K. A. Gonchar, V. S. Marshov, et al., Nanoscale Res. Lett. **7**, 524 (2012).
16. G. Brönstrup, F. Garwe, A. Csaki, et al., Phys. Rev. B **84**, 125432 (2011).
17. Sh. Kato, Y. Kurokawa, Y. Watanabe, et al., Nanoscale Res. Lett. **8**, 216 (2013).
18. L. U. Vinzons, L. Shu, S. Yip, et al., Nanoscale Res. Lett. **12**, 385 (2017).
19. G. K. Mussabek, V. Yu. Timoshenko, K. K. Dikhanbayev, et al., Rec. Contr. Phys. **45**, 14 (2013).
20. B. Franta, E. Mazur, and S. K. Sundaram, Int. Mat. Rev. **63**, 227 (2018).
21. E. Gross, D. Kovalev, N. Kuenzner, et al., Proc. SPIE **5222**, 67 (2003).
22. V. Yu. Timoshenko, Th. Dittrich, V. Lysenko, et al., Phys. Rev. B **64**, 085314 (2001).